

# DIVERSE VARIABILITY OF O AND B STARS REVEALED FROM 2-MINUTES LIGHT CURVES IN SECTORS 1 AND 2 OF THE TESS MISSION: SELECTION OF AN ASTEROSEISMIC SAMPLE

MAY G. PEDERSEN,<sup>1</sup> SOWGATA CHOWDHURY,<sup>2</sup> COLE JOHNSTON,<sup>1</sup> DOMINIC M. BOWMAN,<sup>1</sup> CONNY AERTS,<sup>1,3</sup>  
GERALD HANDLER,<sup>2</sup> PETER DE CAT,<sup>4</sup> CORALIE NEINER,<sup>5</sup> ALEXANDRE DAVID-URAZ,<sup>6</sup> DEREK BUZASI,<sup>7</sup>  
ANDREW TKACHENKO,<sup>1</sup> SERGIO SIMÓN-DÍAZ,<sup>8</sup> EHSAN MORAVVEJI,<sup>9</sup> JAMES SIKORA,<sup>10</sup> GIOVANNI MIROUH,<sup>11</sup>  
CATHERINE C. LOVEKIN,<sup>12</sup> MATTEO CANTIELLO,<sup>13,14</sup> JADWIGA DASZYŃSKA-DASZKIEWICZ,<sup>15</sup> AND ANDRZEJ PIGULSKI<sup>16</sup>

<sup>1</sup>*Instituut voor Sterrenkunde, KU Leuven, Celestijnenlaan 200D, 3001 Leuven, Belgium*

<sup>2</sup>*Nicolaus Copernicus Astronomical Center, Bartycka 18, 00-716 Warszawa, Poland*

<sup>3</sup>*Department of Astrophysics, IMAPP, Radboud University Nijmegen, PO Box 9010, NL-6500 GL Nijmegen, the Netherlands*

<sup>4</sup>*Royal Observatory of Belgium, Ringlaan 3, 1180 Brussel, Belgium*

<sup>5</sup>*LESIA, Paris Observatory, PSL University, CNRS, Sorbonne Université, Univ. Paris Diderot, Sorbonne Paris Cité, 5 place Jules Janssen, 92195 Meudon, France*

<sup>6</sup>*Department of Physics and Astronomy, University of Delaware, Newark, DE 19716, USA*

<sup>7</sup>*Dept. of Chemistry & Physics, Florida Gulf Coast University, 10501 FGCU Blvd. S., Fort Myers, FL 33965 USA*

<sup>8</sup>*(Instituto de Astrofísica de Canarias, 38200 La Laguna, Tenerife, Spain)*

<sup>9</sup>*Facilities for Research, Willem de Croylaan 52c, 3001 Leuven, Belgium*

<sup>10</sup>*Department of Physics, Engineering Physics and Astronomy, Queens University, Kingston, ON K7L 3N6 Canada*

<sup>11</sup>*Astrophysics Research Group, Faculty of Engineering and Physical Sciences, University of Surrey, Guildford GU2 7XH, UK*

<sup>12</sup>*Physics Department, Mount Allison University, Sackville, NB, E4L 1C6, Canada*

<sup>13</sup>*Center for Computational Astrophysics, Flatiron Institute, 162 5th Avenue, New York, NY 10010, USA*

<sup>14</sup>*Department of Astrophysical Sciences, Princeton University, Princeton, NJ 08544, USA*

<sup>15</sup>*Astronomical Institute, University of Wrocław, Kopernika 11, 51-622 Wrocław, Poland*

<sup>16</sup>*Instytut Astronomiczny, Uniwersytet Wrocławski, Kopernika 11, 51-611 Wrocław, Poland*

(Received XXXX; Revised YYYY; Accepted ZZZZ)

Submitted to ApJL

## ABSTRACT

Uncertainties in stellar structure and evolution theory are largest for stars undergoing core convection on the main-sequence. A powerful way to calibrate the free parameters used in the theory of stellar interiors is asteroseismology, which provides direct measurements of interior properties, notably angular momentum and element transport. We report the detection and classification of new variable O and B stars using high-precision short-cadence (2-min) photometric observations assembled by the *Transiting Exoplanet Survey Satellite* (TESS). In our sample of 154 O and B stars, we detect a high percentage (90%) of variability. Among these we find 14 newly discovered multiperiodic pulsators, 6 eclipsing binaries, 21 rotational variables, and 25 stars with stochastic low-frequency variability. Several additional variables overlap between these categories. Our study of O and B stars not only demonstrates the high data quality achieved by TESS for optimal studies of the variability of the most massive stars in the Universe, but also represents the first step towards the selection and composition of a large sample of O and B stars observed with the same telescope and with high potential for joint asteroseismic and spectroscopic modelling of their interior structure with unprecedented precision.

*Keywords:* asteroseismology – stars: massive – stars: evolution – stars: oscillations – stars: rotation – binaries: general

## 1. INTRODUCTION

The variability of stars born with a mass  $M \geq 3M_{\odot}$  is extremely diverse in terms of periodicity (minutes to

centuries) and amplitude ( $\mu\text{mag}$  to  $\text{mag}$ , see e.g. [Aerts et al. 2010](#)). Here, we are concerned with massive stars in the earliest phases of their life, i.e., dwarfs, giants and supergiants, of spectral type O or B. Such stars have a much higher binarity rate than any other spectral type, a phenomenon that cannot be ignored when testing the stellar evolution theory of O and B stars ([Sana et al. 2014](#); [Almeida et al. 2017](#); [Schneider et al. 2018](#)). Throughout their life, these stars are also subject to a strong and stochastically variable radiation-driven wind (e.g. [Lucy & Solomon 1970](#); [Castor et al. 1975](#); [Owocki & Rybicki 1984](#); [Krtićka & Feldmeier 2018](#)).

Compared to other classes of variables, O stars have hardly been monitored with high-precision long-duration space photometry – see Table 3 in [Buysschaert et al. \(2015\)](#) for a summary of space photometric time-series studies of O stars, and more recent studies of their descendants including [Pablo et al. \(2017\)](#); [Johnston et al. \(2017\)](#); [Buysschaert et al. \(2017b\)](#); [Aerts et al. \(2018a\)](#); [Simón-Díaz et al. \(2018a\)](#); [Ramiaramanantsoa et al. \(2018a,b\)](#). Aside from single and multiperiodic pulsational, binary and rotational variability with periods of order hours to weeks, these recent studies also revealed stochastic low-frequency variability. This observed phenomenon was interpreted in terms of internal gravity waves (IGWs) by [Aerts & Rogers \(2015\)](#). The observational signatures of IGWs have meanwhile been investigated systematically from CoRoT and K2 data by [Bowman et al. \(2018\)](#) and [Bowman et al. \(submitted\)](#), respectively, and offers an entirely new way of asteroseismic investigation by bridging 3D hydrodynamical simulations of stochastically excited waves and 1D theory of stellar interiors ([Aerts et al. 2019](#), Fig. 1).

Classical gravity-mode asteroseismology, i.e., forward modelling of the frequencies of coherent identified gravity modes (see [Aerts et al. 2018b](#), for an overview of the methodology), has so far been limited to some 40 stars of spectral type B or F, covering the mass range  $M \in [1.3, 8] M_{\odot}$  and rotation rates from almost zero up to 80% of critical breakup. This revealed the capacity of performing high-precision ( $\sim 10\%$ ) mass estimation of single stars (see [Moravveji et al. 2015, 2016](#); [Szewczuk & Daszyńska-Daszkiewicz 2018](#), for B stars and [Mombarg et al. \(submitted\)](#) for F stars) and of binaries ([Kallinger et al. 2017](#); [Johnston et al. 2019](#)). So far, these asteroseismic studies using space photometry revealed almost rigid rotation for the stars for which estimation of both the near-core ( $\Omega_{\text{core}}$ ) and envelope ( $\Omega_{\text{env}}$ ) rotation could be achieved, following the few earlier results of  $\Omega_{\text{core}}/\Omega_{\text{env}} \in [1, 5]$  from ground-based asteroseismology of early-B stars (see [Aerts 2015](#), for a summary). These asteroseismic findings challenge cur-

rent angular momentum transport theories across the entire mass range ([Aerts et al. 2019](#), their figure 4).

This *Letter* introduces our dedicated study to investigate single and binary O and B stars with the NASA *Transiting Exoplanet Survey Satellite* (TESS) mission ([Ricker et al. 2015](#)). In order to perform asteroseismology, one first needs to find suitable multiperiodic O and B pulsators. We achieve this by classifying the variability of all O and B stars observed by TESS and subsequently selecting those with suitable seismic variability for future modelling. We present our classification and selection strategy for the 2-min cadence light curves obtained in Sectors 1 and 2 of the TESS mission. Accompanying studies focus on the magnetic stars ([David-Uraz et al., in prep](#)) and rotational variability ([Balona et al., submitted](#)) and on a detailed study of the known  $\beta$  Cep star HN Aqr ([Handler et al., submitted](#)).

## 2. METHOD

### 2.1. TESS light curve extraction

To study the variability of massive stars, we analyse a sample of 154 O and B stars observed by TESS with its 2-min cadence, out of which 40 are located in the LMC. These 154 stars were identified as O and B stars based on the spectral types provided in SIMBAD<sup>1</sup>.

The data treated here were obtained by TESS in Sectors 1 (July 25 – Aug 22, 2018) and 2 (2018, Aug 23 – Sept 20) and are publicly available via the Mikulski Archive for Space Telescopes (MAST)<sup>2</sup>. The extracted time series are in the format of reduced Barycentric Julian Date (BJD – 2457000) and stellar magnitudes, where the latter have been adjusted to show variability around zero by subtracting the mean. Where necessary, we performed detrending of long-term instrumental effects by means of subtracting a linear or low-order polynomial fit to a sector.

### 2.2. Classification procedure

We calculated amplitude spectra of all light curves using Discrete Fourier Transforms (DFT) following the method by [Kurtz \(1985\)](#). We used an oversampling factor of ten to ensure that all frequency peaks in the DFT are adequately resolved. The 2-min cadence of TESS results in a Nyquist frequency of  $360 \text{ d}^{-1}$ , which is sufficiently high to avoid a bias when extracting significant frequencies using iterative prewhitening. Amplitude suppression of variability in time series is negligible within the frequency range of interest for such high

<sup>1</sup> <http://simbad.u-strasbg.fr/simbad/>

<sup>2</sup> [http://archive.stsci.edu/tess/all\\_products.html](http://archive.stsci.edu/tess/all_products.html)

sampling (Bowman 2017). Based on visual inspection of the light curves and amplitude spectra by several of the authors independently, we provide the variability classification of all 154 O and B stars in Table 1 in Appendix A. We also report the number of available spectra for each of the stars and the instrument used for the observations. This information is particularly relevant for future studies of these 154 O and B stars and are reported here for completeness. Figures of the light curves and amplitude spectra are made available electronically in Appendix B.

### 2.3. Gaia color-magnitude diagram

Asteroseismic modelling of stars with coherent oscillation modes can be optimally performed if at least one additional global stellar parameter (aside from the identified oscillation frequencies) can be measured with high precision. The availability of such an independent measurement helps greatly to break degeneracies among the global and local stellar model parameters to be estimated (e.g., Moravveji et al. 2015, Figs 5 and B.1). A model-independent mass from binarity (Johnston et al. 2019) or a high-precision (10%) spectroscopic estimate of the effective temperature (Mombarg et al., submitted) have been used to break degeneracies. Another useful quantity is a star’s luminosity from Gaia data (Pedersen et al., in preparation).

With this in mind, and to check the SIMBAD spectral types that went into the selection of our sample, we used Gaia DR2 photometry (Gaia Collaboration et al. 2018a) to place all our sample stars in a color-magnitude diagram (CMD, Fig. 1). Each star was color-coded by its dominant variability type. The apparent Gaia G-band magnitudes were converted to absolute magnitudes  $M_G$  using the Gaia DR2 distances from Bailer-Jones et al. (2018). The colours are derived from the apparent Gaia BP and RP band magnitudes. All other stars observed in 2-min cadence by TESS in Sectors 1 and 2 with Gaia DR2 data available were included (20883 out of the 24816 TESS targets indicated by black dots). Using the same approach as in Gaia Collaboration et al. (2018b), the position of the stars in Fig. 1 have not been corrected for reddening or extinction, but we show a typical  $2\sigma$  error bar for the positioning of the stars in the CMD. Two stars (TIC 197641601 = HD 207971 and TIC 354671857 = HD 14228) are outliers in the CMD (at BP-RP > 2). Although these stars are B stars, they are bright ( $V = 3.01$  and  $3.57$ , respectively) which could explain the discrepant Gaia photometry. Furthermore, based on the position in the CMD we excluded two stars (TIC 206482194 = HE 2203-2210 and TIC 290648723 = EC 00311-8215) from our original sample of 156 stars,

as they turn out to be sdB stars. These stars are not counted in the 154 number of stars reported in this work.

The 151 out of 154 stars in our sample observed with Gaia shown in color in Fig. 1 constitute the first sample of variable O and B stars monitored at high cadence in high-precision space photometry, after the K2 sample monitored at 30-min cadence in Bowman et al. (submitted). These two samples, along with future ones assembled by the TESS mission, will reveal numerous O and B stars suitable for asteroseismic modelling. Such modelling requires a frequency precision better than  $0.001 \text{ d}^{-1}$  and pulsation mode identification for tens of modes (Aerts et al. 2018b). In this way, we will extend the large *Kepler* samples of hundreds of low-mass and intermediate-mass pulsators with estimation of their interior rotation profile discussed in Aerts et al. (2019) to higher masses. The interior physics, and rotation and chemical mixing profiles in particular, will hence be calibrated asteroseismically for large samples of massive stars that eventually explode as supernovae.

## 3. RESULTS

It is not possible to discuss each star in the sample individually. Here we focus on the binarity and pulsational properties, and briefly discuss the detection of rotational and/or magnetic properties of the sample of stars. Out of a total of 154 stars, 41 show clear variability in their light-curves but their nature could not be uniquely identified.

### 3.1. Eclipsing binaries

Eclipsing binaries (EBs) hold the potential to provide model-independent distance, radius, and mass estimates and are crucial calibrators for stellar evolutionary theory (Torres et al. 2010, for a review). Unfortunately, the number of O and B stars in EBs observed with high-precision space photometry remains small compared to the thousands of binaries with low-mass components (Kirk et al. 2016).

Six of the stars in our sample were already known as EBs and we confirm this classification using the TESS data: HD 6882 ( $\zeta$  Phe), HD 61644 (V455 Car), HD 224113 (AL Scl), HD 42933 ( $\delta$  Pic), HD 31407 (AN Dor), and HD 46792 (AE Pic). Their light curves in Appendix B are of unprecedented quality and future modelling will improve their mass determinations. One of these stars (HD 42933) is known to have  $\beta$  Cep type pulsations detected from BRITE photometry (Pigulski et al. 2017). We confirm the variability in this work. In addition, the three objects (HD 224990, HD 269382 and HD 53921) were known spectroscopic binaries, while ten more (HD 269676, HD 68520, HD 19400, HD 53921,

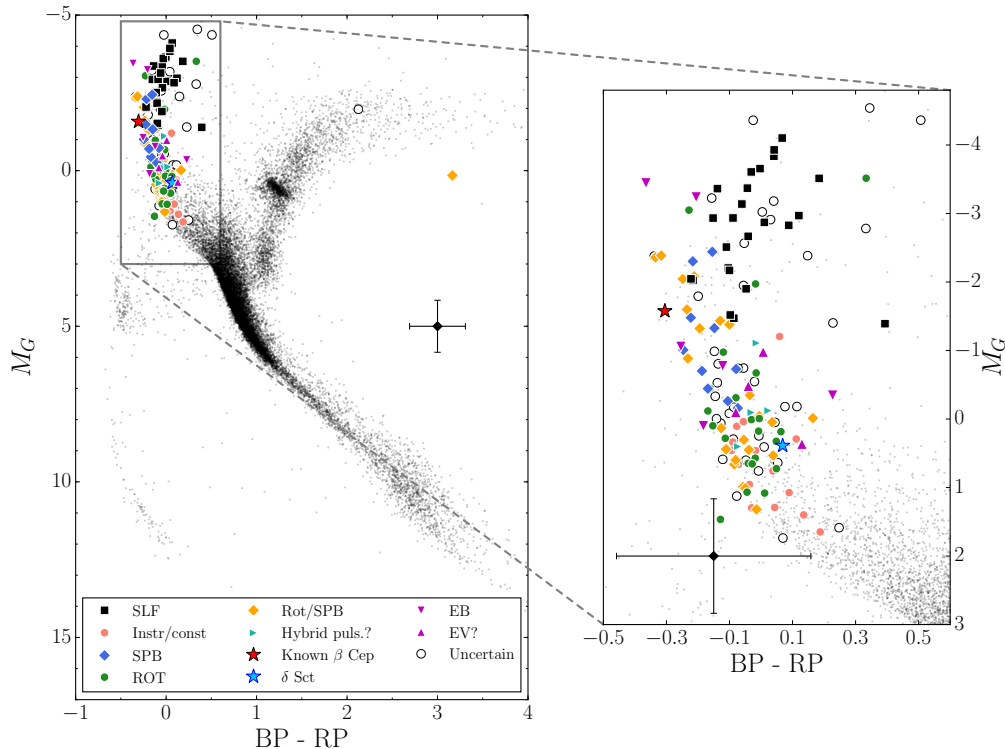


**Figure 1.** Classification results for O and B stars placed in a Gaia DR2 CMD. Black dots are the entire TESS sector 1 and 2 short-cadence stars also observed by Gaia, and open black circles corresponds to uncertain classification. The labels in the legend correspond to the following types of variability: SLF = Stochastic low-frequency signal, Instr/const = possibly instrumental or constant, SPB = slowly pulsating B star, ROT = rotational modulation, ROT/SPB = rotational modulation and/or SPB, Hybrid puls.? = both p- and g-modes, EB = Eclipsing Binary, EV? = Ellipsoidal variable or rotational modulation,  $\delta$  Sct =  $\delta$  Scuti star. The error bar shows a typical  $2\sigma$ -error on the position in the CMD, shown in both panels for convenience.

HD 2884, HD 46860, HD 208433, HD 37854, HD 209014 and CPD-60 944) were listed as known double or multiple stars in SIMBAD; the TESS light curves of these 13 non-eclipsing binaries did not reveal the binarity, except for HD 208433, which shows the signature of a single transit. In addition to the eclipsing binaries, we find four stars showing either ellipsoidal variation or rotational modulation from spots: HD 268798, HD 222847, HD 20784 and HD 37935. None of these four stars have previously been identified as binaries, but HD37935 is a known Be star.

HD 53921 is a known spectroscopic magnetic binary, which was previously identified as a Slowly Pulsating B (SPB) star by De Cat & Aerts (2002). However, with the help of the high-quality TESS light curves we find that the reported dominant g-mode frequency of  $0.6054 \text{ d}^{-1}$  shows a second harmonic. Based on this as well as the morphology of the light curve, we deduce that this frequency is caused by rotational modulation from magnetic spots. This example illustrates how difficult g-mode asteroseismology from ground-based observations can be. This and other known magnetic stars in the

sample are discussed in more detail in David-Uraz et al. (in prep.).

In total, the light curves of eight of these 19 binaries reveal pulsations. We show the phased light curve for a newly discovered binary pulsator (HD 61644=TIC 349907707) in Fig. 2. This result illustrates the promise of TESS to provide numerous pulsating O and B binaries suitable to calibrate stellar evolution models from binary asteroseismology (Johnston et al. 2019).

### 3.2. Pulsating stars

Coherent non-radial oscillation modes in O and B stars come in two main flavors: pressure modes with periods of a few hours ( $\beta$  Cep stars, for spectral types from O9 to B3) and gravity modes with periods of order a few days (SPB stars, for spectral types from late O to B9). For an extensive discussion on their early discoveries and pulsation properties, we refer to Aerts et al. (2010, Chapter 2). However, the space-based photometry assembled with MOST, CoRoT, *Kepler*, K2, and BRITe revealed that many O and B pulsators are *hybrids*, i.e., pulsators with both types of modes simul-

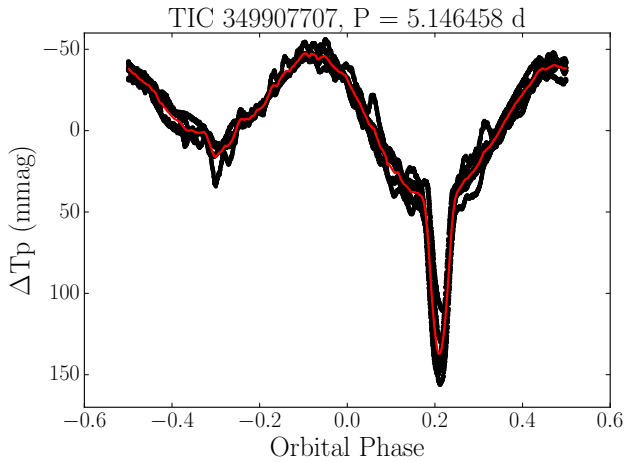


**Figure 2.** Phase folded light curve (black) of the known eclipsing binary HD 61644, showing the signature of previously unknown pulsations. The red line shows the binned phase curve. The pulsational signal is seen on top of this.

taneously, with the dominant type of pulsation being determined by the spectral type, as outlined above. Such hybrid pulsators have proven to be a powerful tool for constraining and studying opacities in the partial ionization layers responsible for exciting the pulsations. As an example, the detailed seismic modelling of  $\nu$  Eri performed by Daszyńska-Daszkiewicz et al. (2017) revealed that a factor three increase in the opacity at  $\log T = 5.46$  was needed to excite the g-modes in this star.

In total, we find 14 new O and B pulsators, among which 10 have gravity modes and four are potential hybrids. We show the light curves and DFTs for one of the newly discovered SPB and hybrid stars in Fig 3 and Fig 4, respectively. One star in the sample, HN Aqr, is a known  $\beta$  Cep star and is discussed in Handler et al. (submitted). Future continued TESS and/or spectroscopic monitoring will be needed to assess the asteroseismic potential of these 14 pulsators in terms of frequency precision and mode identification.

### 3.3. Rotational variability

We classified 21 of the stars in our sample as rotational variables, one of which is labeled as a Wolf Rayet star in SIMBAD (HD 269582). Among these are four stars previously known to be magnetic: HD 223640 (Bychkov et al. 2005; Sikora et al. 2018), HD 53921 (Hubrig et al. 2006; Bagnulo et al. 2015) and HD 63204 (Bernhard et al. 2015; Hümmerich et al. 2016), as well as HD 65987 (Bagnulo et al. 2015). Rotational modulation is usually interpreted as due to temperature and/or chemical spots on the stellar surface caused by large-scale magnetic fields. We refer to the accompanying papers by David-Uraz et al. (in prep.) and Balona et al. (submitted) for an

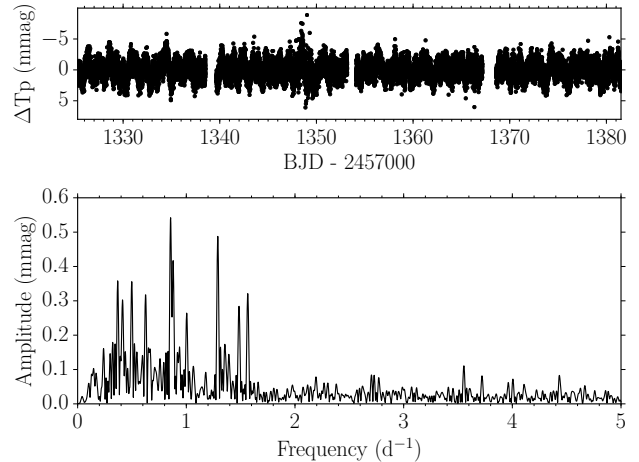


**Figure 3.** Example of a newly-discovered SPB star (TIC 167523976 = HD 49193). The TESS light curve and amplitude spectrum are shown in the top and bottom panels, respectively.

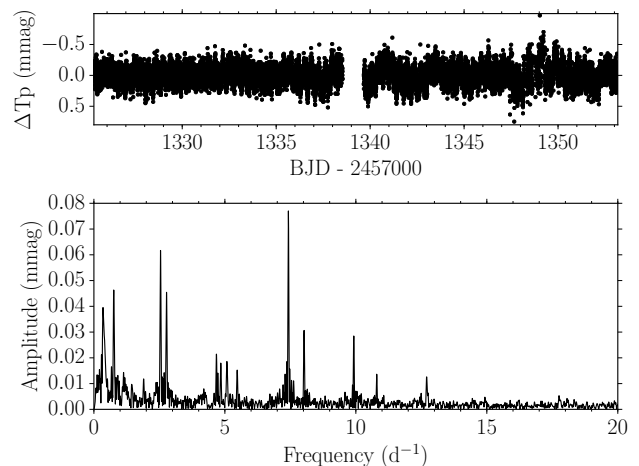


**Figure 4.** Example of a newly-discovered hybrid pulsator showing both SPB and  $\beta$  Cep type pulsations (TIC 469906369 = HD 212581). The TESS light curve and amplitude spectrum are shown in the top and bottom panels, respectively.

extensive discussion of the rotational modulation and magnetic properties of the sample.

The star HD 10144 (aka Achernar and  $\alpha$  Eri) is a Be star rotating at 95% of critical breakup, whose stellar disk has been imaged by interferometry (Dalla Vedova et al. 2017). We find its dominant frequency to be  $0.729 \text{ d}^{-1}$ . Also HD 214748, HD 209522, HD 33599, HD 19818, HD 221507, HD 46860, HD 37974, HD 53048, CD-56 152, HD 209014, HD 37935, HD 68423, HD 224686 and HD 66194 were known to be Be stars prior to our study. However, while HD 221507 is known as a Be star, recent studies have shown that it lacks

clear emission and has a low  $v \sin i$  (e.g. [Arcos et al. 2017](#)).

In addition to the stars classified as rotational variables, we found 25 stars which show rotational modulation and/or SPB type variability. The simultaneous occurrence of rotation and pulsation frequencies in space photometry is not unusual, but there is only one such case so far for which combined spectropolarimetric and asteroseismic modelling has been achieved: the hybrid magnetic  $\beta$  Cep/SPB star HD 43317 monitored by CoRoT ([Buysschaert et al. 2017a, 2018](#)). Our results are encouraging to expand the domain of magneto-asteroseismology in the near future.

### 3.4. Stochastic, low-frequency signatures

Stochastic, low-frequency (SLF) variability has recently been shown to be a common phenomenon in blue supergiants in both space-based photometry ([Bowman et al. 2018](#)) and spectroscopy ([Simón-Díaz et al. 2018b](#)). Several theories have been offered to explain this variability, such as sub-surface convection, dynamical stellar winds and IGWs excited at the convective core boundary (see [Bowman et al. 2018](#), for a detailed discussion). In our sample of 154 O and B stars, we find 25 stars with stochastic low-frequency variability, all of which are classified as blue supergiants based on the spectral types from SIMBAD. This is in agreement with the conclusions by [Bowman et al.](#) (submitted) from K2 photometry of such stars.

### 3.5. Other types of variability

We found several stars in our sample that showed “outbursts” in their light curves (see [Table 1](#) and [Appendix B](#)). Such outbursts may be connected with episodic mass loss, such as in Be stars, or flaring due to magnetic activity in low-mass stars. In some cases, the detected outbursts occur in various of the light curves at the same time and for the same duration. This is a strong indication that for these stars the signature is likely instrumental. For the remainder of the targets, spectroscopic follow-up and a study of the pixel data is required to confirm that the outbursts are physical, rather than instrumental artefacts ([Pedersen et al. 2017](#)). A more extensive discussion is provided in [Balona et al.](#) (submitted).

## 4. DISCUSSION AND CONCLUSIONS

We presented stellar variability classification for the 154 stars with spectral type O or B that were monitored in short-cadence (2-min) by the TESS mission in its Sectors 1 and 2. We found 138 of the O and B dwarfs, giants, and supergiants to be variable at the TESS detection threshold. This is a high percentage of variability

(90%) given that the time base of each sector is only 27 d, preventing longer-period variables from being discovered. We placed the 151 out of 154 targets with a Gaia DR2 parallax in a CMD ([Fig. 1](#)).

Our variability classification had the main goal to start compiling an optimal large and unbiased sample of O and B stars for future asteroseismology, either based on multiple individual frequencies of identified coherent standing modes and/or from the observed properties of low-frequency stochastically excited IGWs. We found 15 single and 8 binary O and B pulsators (i.e., altogether 15% of the monitored stars) as potential candidates for such future asteroseismic modelling, and 25 stars with stochastic, low-frequency signatures (16%). Among these, the 79 stars in the continuous viewing zone are the most promising for asteroseismic modelling. However, for all of them, an extension of the TESS light curve monitoring will provide the frequency precision required for such detailed modelling efforts. Our initial study thus reveals the major potential of the combined TESS, Gaia, and spectroscopic all-sky monitoring as already outlined by [Kollmeier et al. \(2017\)](#).

*Acknowledgments:* The research leading to these results has received funding from the European Research Council (ERC) under the European Union’s Horizon 2020 research and innovation program (grant agreement No. 670519: MAMSIE). This paper includes data collected by the TESS mission. Funding for the TESS mission is provided by the NASA Explorer Program. Funding for the TESS Asteroseismic Science Operations Centre is provided by the Danish National Research Foundation (Grant agreement no.: DNRFF106), ESA PRODEX (PEA 4000119301) and Stellar Astrophysics Centre (SAC) at Aarhus University. We thank the TESS and TASC/TASOC teams for their support of the present work. This research has made use of the SIMBAD database, operated at CDS, Strasbourg, France. Some of the data presented in this paper were obtained from the Mikulski Archive for Space Telescopes (MAST). STScI is operated by the Association of Universities for Research in Astronomy, Inc., under NASA contract NAS5-2655. GH and SC thanks the Polish NCN for support (grant 2015/18/A/ST9/00578). AT acknowledges support from the Research Foundation Flanders (FWO) under the grant agreement G0H5416N (ERC runner-up grant). JDD acknowledges support from the NCN grant no. 2015/17/B/ST9/02082. APi acknowledges support from the NCN grant no. 2016/21/B/ST9/01126. ADU gratefully acknowledges support from the Natural Science and Engineering Research Council (NSERC) of Canada.

## REFERENCES

- Aerts, C. 2015, in IAU Symposium, Vol. 307, New Windows on Massive Stars, ed. G. Meynet, C. Georgy, J. Groh, & P. Stee, 154–164
- Aerts, C., Christensen-Dalsgaard, J., & Kurtz, D. W. 2010, *Asteroseismology*, Astronomy and Astrophysics Library, Springer-Verlag, Heidelberg
- Aerts, C., Mathis, S., & Rogers, T. 2019, *ARA&A*, in press, arXiv:1809.07779
- Aerts, C., & Rogers, T. M. 2015, *ApJL*, 806, L33
- Aerts, C., Bowman, D. M., Símón-Díaz, S., et al. 2018a, *MNRAS*, 476, 1234
- Aerts, C., Molenberghs, G., Michielsen, M., et al. 2018b, *ApJS*, 237, 15
- Almeida, L. A., Sana, H., Taylor, W., et al. 2017, *A&A*, 598, A84
- Arcos, C., Jones, C. E., Sigut, T. A. A., Kanaan, S., & Curé, M. 2017, *ApJ*, 842, 48
- Bagnulo, S., Fossati, L., Landstreet, J. D., & Izzo, C. 2015, *A&A*, 583, A115
- Bailer-Jones, C. A. L., Rybizki, J., Fousneau, M., Mantelet, G., & Andrae, R. 2018, *AJ*, 156, 58
- Bernhard, K., Hümmerich, S., Otero, S., & Paunzen, E. 2015, *A&A*, 581, A138
- Bowman, D. M. 2017, *Amplitude Modulation of Pulsation Modes in Delta Scuti Stars*, doi:10.1007/978-3-319-66649-5
- Bowman, D. M., Aerts, C., Johnston, C., et al. 2018, *A&A*, in press (arXiv1811.08023), arXiv:1811.08023
- Buysschaert, B., Aerts, C., Bowman, D. M., et al. 2018, *A&A*, 616, A148
- Buysschaert, B., Neiner, C., Briquet, M., & Aerts, C. 2017a, *A&A*, 605, A104
- Buysschaert, B., Aerts, C., Bloemen, S., et al. 2015, *MNRAS*, 453, 89
- Buysschaert, B., Neiner, C., Richardson, N. D., et al. 2017b, *A&A*, 602, A91
- Bychkov, V. D., Bychkova, L. V., & Madej, J. 2005, *A&A*, 430, 1143
- Castor, J. I., Abbott, D. C., & Klein, R. I. 1975, *ApJ*, 195, 157
- Dalla Vedova, G., Millour, F., Domiciano de Souza, A., et al. 2017, *A&A*, 601, A118
- Daszyńska-Daszkiewicz, J., Pamyatnykh, A. A., Walczak, P., et al. 2017, *MNRAS*, 466, 2284
- De Cat, P., & Aerts, C. 2002, *A&A*, 393, 965
- Gaia Collaboration, Brown, A. G. A., Vallenari, A., et al. 2018a, *A&A*, 616, A1
- Gaia Collaboration, Eyer, L., Rimoldini, L., et al. 2018b, *A&A*, in press, arXiv:1804.09382
- Hubrig, S., North, P., Schöller, M., & Mathys, G. 2006, *Astronomische Nachrichten*, 327, 289
- Hümmerich, S., Paunzen, E., & Bernhard, K. 2016, *AJ*, 152, 104
- Johnston, C., Buysschaert, B., Tkachenko, A., Aerts, C., & Neiner, C. 2017, *MNRAS*, 469, L118
- Johnston, C., Tkachenko, A., Aerts, C., et al. 2019, *MNRAS*, 482, 1231
- Kallinger, T., Weiss, W. W., Beck, P. G., et al. 2017, *A&A*, 603, A13
- Kirk, B., Conroy, K., Prša, A., et al. 2016, *AJ*, 151, 68
- Kollmeier, J. A., Zasowski, G., Rix, H.-W., et al. 2017, *SDSS-V White Paper*, arXiv1711.03234, arXiv:1711.03234
- Krtićka, J., & Feldmeier, A. 2018, *A&A*, 617, A121
- Kurtz, D. W. 1985, *MNRAS*, 213, 773
- Lucy, L. B., & Solomon, P. M. 1970, *ApJ*, 159, 879
- Moravceji, E., Aerts, C., Pápics, P. I., Triana, S. A., & Vandoren, B. 2015, *A&A*, 580, A27
- Moravceji, E., Townsend, R. H. D., Aerts, C., & Mathis, S. 2016, *ApJ*, 823, 130
- Owocki, S. P., & Rybicki, G. B. 1984, *ApJ*, 284, 337
- Pablo, H., Richardson, N. D., Fuller, J., et al. 2017, *MNRAS*, 467, 2494
- Pedersen, M. G., Antoci, V., Korhonen, H., et al. 2017, *MNRAS*, 466, 3060
- Pigulski, A., Jerzykiewicz, M., Ratajczak, M., Michalska, G., & Zahajkiewicz, E. 2017, in *Second BRITE-Constellation Science Conference: Small satellites—big science*, Proceedings of the Polish Astronomical Society volume 5, held 22-26 August, 2016 in Innsbruck, Austria. Edited by Konstanze Zwintz and Ennio Poretti. Polish Astronomical Society, Bartycka 18, 00-716 Warsaw, Poland, pp.120-127, ed. K. Zwintz & E. Poretti, 120–127
- Ramiamananantsoa, T., Ratnasingam, R., Shenar, T., et al. 2018a, *MNRAS*, 480, 972
- Ramiamananantsoa, T., Moffat, A. F. J., Harmon, R., et al. 2018b, *MNRAS*, 473, 5532
- Ricker, G. R., Winn, J. N., Vanderspek, R., et al. 2015, *Journal of Astronomical Telescopes, Instruments, and Systems*, 1, 014003
- Sana, H., Le Bouquin, J.-B., Lacour, S., et al. 2014, *ApJS*, 215, 15
- Schneider, F. R. N., Sana, H., Evans, C. J., et al. 2018, *Science*, 359, 69
- Sikora, J., Wade, G. A., Power, J., & Neiner, C. 2018, *MNRAS*, arXiv:1811.05635

Simón-Díaz, S., Aerts, C., Urbaneja, M. A., et al. 2018a,  
A&A, 612, A40  
—. 2018b, A&A, 612, A40  
Szewczuk, W., & Daszyńska-Daszkiewicz, J. 2018, MNRAS,  
478, 2243

Torres, G., Andersen, J., & Giménez, A. 2010, A&A Rv,  
18, 67

## APPENDIX

## A. VARIABILITY CLASSIFICATION

In Table 1, we provide the TESS Input Catalogue (TIC) and Gaia identification numbers, as well as Gaia magnitudes and colours, **SIMBAD** spectral types and the classification of the dominant source(s) of variability for each of the 154 O and B stars observed by TESS in sectors 1 and 2 at a 2-min cadence.

**Table 1.** Identification numbers, parameters and variability classification of the 154 O and B stars. EB = eclipsing binary, EV = ellipsoidal variable, rot = Rotational modulation, SPB,  $\beta$  Cep, SLF = stochastic low-frequency signal, instr = instrumental, const = constant, puls = pulsational signal not clearly identified in any of the previous categories, and  $\delta$  Sct =  $\delta$  Scuti star. We provide an overview of which stars have spectra available. U = UVES, F = FEROS, X = X-SHOOTER, E = ESPRESSO

TIC	Name	Sp. Type SIMBAD	Gaia DR2 ID	$M_G$ (mag)	BP - RP (mag)	# Spectra	Instrument	Var. Type
12359289	HD 225119	Apsi	2333119869770412288	-0.98	-0.12	1	F	rot
29990592	HD 268623	B2Ia	4657589254497529344	-4.10	0.07	1	F	SLF
30110048	HD 268653	B3Ia	4765410903770283008	-2.02	-0.22	1	F	SLF
30268695	HD 268809	B1Ia	5290767631226220032	-2.20	-0.10	1	F	SLF
30275662	Sk-66 27	B3Ia	4661771801060664064	-3.37	-0.04	4	U	SLF
30275861	[HT83] alf	O6V	4662155839823561216	1.47	-0.13	?	?	rot
30312676	HD 268726	B2Ia	4662153812635167488	-2.87	0.01	2	U	SLF
30312711	BI 42	O8V	-	-	-	?	?	SLF / rot / EB?
30317301	HD 268798	B2Ia	4661511422956353152	-3.02	0.00	-	-	EV / rot / SLF
30933383	Sk-68 39	B2.5Ia	4662153469001983104	-2.97	0.12	2	F	SLF
31105740	TYC 9161-925-1	B0.5Ia	4655458160445111552	-2.93	-0.15	1/3	F/U	SLF
31181554	HD 269050	B0Ia	4661392533937464448	-2.05	-0.22	22/12	X/U	SLF
31867144	HD 22252	B8IV	4671120982756449664	-1.11	-0.01	-	-	rot / SPB + $\beta$ Cep hybrid?
33945685	HD 223118	B9.5V	2338752697903817216	1.29	0.04	-	-	instr? ( $\nu_{\text{inst}} \simeq 2.8 \text{ d}^{-1}$ )/puls
38602305	HD 27657 AB	B9IV	4676067719930656640	0.28	-0.11	-	-	rot
40343782	HD 269101	B3Iab	5288240197589081728	-3.18	0.04	-	-	SLF / SPB?
41331819	HD 43107	B8V	5282761464287879296	0.29	-0.09	84/12	X/U	rot / outburst?
47296054	HD 214748	B8Ve	6622561673163632768	-1.38	-0.10	26	U	rot / SPB / Be
49687057	HD 220787	B3III	4657674745869490304	-2.38	0.15	6/18	F/X	instr / binary?
53992511	HD 209522	B4Ive	2436569757731466112	-2.04	-0.25	3/18/1/15	F/X/E/U	rot / SPB / Be
55295028	HD 33599	B2Vpe	6619440159652409728	-1.60	-0.23	1	F	rot / SPB / Be
66497441	HD 222847	B9V	2391220091406075648	-0.10	-0.08	1/42	F/U	EV / rot? / SPB?
69925250	V* HN Aqr	B	2402031280004432512	-1.58	-0.30	4	U	known $\beta$ Cep
89545031	HD 223640	A0VpSiSr	2390144081839340288	0.10	-0.15	33	U	rot
92136299	HD 222661 A	B9V	2419885149815948416	0.99	-0.06	28	U	SPB+Be-type mini-outbursts / rot
115177591	HD 201108	B8IV/V	6775980889978989824	-0.16	-0.07	-	-	SPB

Table 1 continued

Table 1 (continued)

TIC	Name	Sp. Type SIMBAD	Gaia DR2 ID	$M_G$ (mag)	BP - RP (mag)	# Spectra	Instrument	Var. Type
139468902	HD 213155	B9.5V	6521195703338406272	1.01	-0.05	1/63/1	F/X/U	rot / SPB?
141281495	HD 37854	B9/9.5V	4648666996817764736	0.57	-0.02	-	-	rot?
149039372	HD 34543	B8V	4663645952980782848	0.30	-0.05	-	-	rot? / SPB?
149971754	HD 41297	B8Ib	5482011113182765696	-0.26	-0.11	-	-	SPB
150357404	HD 45796	B6V	5477233430220256384	-0.44	-0.17	1	F	SPB
150442264	HD 46792	B2V	4760693797025929344	-3.24	-0.21	-	-	EB + puls/rot
152283270	HD 208433	B9.5V	6588214059487740672	0.25	-0.01	-	-	instr / binary(transit)
167045028	HD 45527	B9IV	5279546835885790720	0.01	-0.03	-	-	rot
167415960	HD 48467	B8/9V	5266733784509615616	0.11	-0.08	1	F	const?
167523976	HD 49193	B2V	4660166788974686976	-1.48	-0.22	-	-	SPB
176935619	HD 49306	B9.5/A0V	5280155179351701504	1.02	-0.05	-	-	instr? ( $\nu_{\text{inst}} \approx 2.8 \text{ d}^{-1}$ )
176955379	HD 49531	B8/9Vn	5279020208473101056	0.45	-0.04	-	-	SPB / rot
177075997	HD 51557	B7III	5266581089830743296	-0.99	-0.15	1	F	instr / rot?
179308923	HD 269882	O9.5Ib	4657651857940816640	-2.57	-0.05	-	-	SLF? / SPB?
179574710	HD 271213	B1Iak	4661778810447390720	-1.47	-0.09	-	-	SLF
179637387	[OM95] LH 47-373A	B1Ia	4651354886129065600	-1.52	-0.10	-	-	SLF
179639066	HD 269440	B1Ib	4658741370886084992	-2.17	-0.10	2	F	SLF
182909257	HD 6783	Ap Si	4635279171434162304	0.65	-0.04	-	-	rot
197641601	HD 207971	B8IV-Vs	6586825380598277248	-1.97	2.13	22	U	instr / rot
206362352	HD 223145	B3V	5283754052709233920	-2.30	-0.22	1/3/302	F/X/U	SPB
206547467	HD 210780	B9.5/A0	6819470079550296960	1.74	0.07	-	-	rot / const? / SPB?
207176480	HD 19818	B9/A0Vn(e)	4723685987980665088	1.59	0.25	3	F	SPB? / SLF? / Be
207235278	HD 20784	B9.5V	4733510055655723392	-0.98	0.01	-	-	EV / rot
220430912	HD 31407	B2/3V	6522301330997312128	-1.06	-0.25	84	X	EB + puls
224244458	HD 221507	B9.5IIIpHgMnSi	6538585991555664128	0.59	-0.12	3/30	F/U	rot + mini-outburst?
229013861	HD 208674	B9.5V	6612822091790516480	1.07	-0.04	-	-	rot
230981971	HD 10144	B6Vpe	-	-	-	217/270	F/U	rot / SPB? / Be
231122278	HD 29994	B8/9V	4656238611846958208	0.53	0.04	-	-	rot / SPB?
238194921	HD 24579	B7III	4627113682690040576	-0.35	-0.04	-	-	rot / SPB
259862349	HD 16978	B9Va	4695167130257150592	0.66	-0.07	6/9/20	F/X/U	instr

Table 1 continued

Table 1 (continued)

TIC	Name	Sp. Type SIMBAD	Gaia DR2 ID	$M_G$ (mag)	BP - RP (mag)	# Spectra	Instrument	Var. Type
260128701	HD 42918	B4V	5494534348761557888	-1.01	-0.25	-	-	SPB
260131665	HD 42933	B1/2(III)n	5499415974230271488	-3.45	-0.36	4	F	EB + $\beta$ Cep
260368525	HD 44937	B9.5V	5494983804202264192	-0.18	0.11	-	-	SPB?
260540898	HD 46212	B8IV	5496276314480471040	-0.55	-0.02	-	-	rot?
260640910	HD 46860 AB	B9IVn+A8V;p?	5482771807727582080	-0.73	-0.08	2	F	SPB/Be
260820871	HD 218801	B9.5V(n)	6381543153782126464	0.60	-0.05	-	-	rot / binary?
261205462	HD 40953	B9V	4623532264081294464	0.66	-0.08	1	F	SPB / rot
262815962	HD 218976 AB	B9.5/A0V	6500025053617700992	1.32	-0.01	-	-	rot / SPB?
270070443	HD 198174	B8II	6805364208656989696	-0.31	-0.08	-	-	rot
270219259	HD 209014 AB	B8/9V+B8/9	6617682865193265536	-1.40	0.23	3	F	instr / $\beta$ Cep + outburst
270557257	HD 49835	B9.5V	5211969859107211136	1.40	0.14	-	-	instr ( $\nu_{\text{inst}} \simeq 2.8 \text{ d}^{-1}$ )
270622440	HD 224112	B8V	2314214110928211712	-0.08	-0.10	3	F	EB (contamination!)
270622446	HD 224113	B5/8	2314213698611350144	-0.78	-0.12	36/18	F/X	EB
271503441	HD 2884 AB	B8/A0	4900927434176620160	1.12	-0.08	11	F	SPB? / outburst?
271971626	HD 62153 AB	B9IV	5214590201474858624	-0.01	-0.01	-	-	rot
276864600	HD 269777	B3Ia	4661270350708775296	-1.90	-0.05	5	F	SLF
277022505	HD 269786	BII	4657274283151403520	-3.66	-0.00	-	-	SLF
277022967	HD 37836	B0e(q)	4657280639705552768	-4.54	0.34	12/70	F/X	rot / SPB? / SLF? / Be
277099925	HD 269845	B2.5Ia	4661439439319405184	-2.67	-0.04	-	-	SLF
277103567	HD 37935	B9.5V	4660284883361750912	-0.48	-0.04	2/30	F/X	rot / EV?
277172980	HD 37974	B0.5e	4657658356271368064	-4.36	0.51	11/6	F/X	SLF? / Be
277173650	HD 269859	BIIa	4658882353222625920	-3.23	-0.16	40	X	SLF / instr?
277298891	Sk-69 237	BIIa	465769659311713024	-1.39	0.39	1	F	SLF
277982164	HD 54239	B9.5/A0III/IV	5211241295215037696	-0.01	0.16	36	U	rot / SPB
278683664	HD 47770	B9.5V	5484286625513030016	0.76	0.04	-	-	const??
278865766	HD 48971	B9V	5496814662861807360	0.46	-0.02	-	-	const??
278867172	HD 49111	B9.5V	5497973449334379904	0.96	-0.04	-	-	const??
279430029	HD 53048	B5/7Vn(e)	5484134029618653952	-1.97	-0.02	-	-	rot / Be
279511712	HD 53921 AB	B9III+B8V	5480486644608749696	-0.12	-0.17	-	-	rot
279957111	HD 269582	WN10h	4658481718680657792	-3.51	0.33	211	X	rot

Table 1 continued

Table 1 (continued)

TIC	Name	Sp. Type SIMBAD	Gaia DR2 ID	$M_G$ (mag)	BP - RP (mag)	# Spectra	Instrument	Var. Type
280051467	HD 19400 AB	B8III/IV	4645479443883933824	-0.45	-0.16	1/238	F/U	rot
280684074	HD 215573	B6V	635188232009033248	-0.70	-0.19	1/8	F/U	SPB
281703963	HD 4150 A	A0IV	4908022136034353152	-0.12	0.02	1	F	hybrid SPB/ $\delta$ Sct
281741629	CD-56 152	Be	4908668373993964032	-3.05	-0.23	2/6	F/U	rot / Be
293268667	HD 47478	B9V	5477090356269215616	0.60	-0.08	-	-	SPB/ rot?
293973218	HD 54967	B4V	5478303942228108288	-2.08	-0.21	-	-	rot / SPB
294747615	HD 30612	B8II/III(pSi)	4654833539071572736	-0.33	-0.15	1	F	rot / SLF?
294872353	HD 270754	B1.5Ia	4657655435693905408	-4.36	-0.02	1/20	F/U	SLF?
300010961	HD 55478	B8III	5280667689208638976	-0.00	-0.14	-	-	rot / $\beta$ Cep ?
300325379	HD 58916	B1.5Ia	5281254278662916736	0.41	0.01	-	-	rot?
300329728	HD 59426	B9V	5267524573886888320	0.72	0.05	-	-	rot
300744369	HD 63928	B9V	5270696836731782144	1.08	0.01	-	-	rot
300865934	HD 64484	B9V	5275049837626917504	0.04	-0.06	-	-	instr / outburst?
306672432	HD 67252	B8/9V	5271283391825477248	0.76	-0.01	-	-	const? / rot?
306824672	HD 68221	B9V	5270992635422817792	0.05	0.04	-	-	rot? / SPB?
306829961	HD 68520 AB	B5III	5270986008289935232	-2.44	-0.15	-	-	SPB
307291308	HD 71066	B9/A0IV	5221286296008492416	0.06	-0.13	13	U	instr / rot?
307291318	HD 71046 AB	B9III/IV	5221286158569529344	-0.17	-0.09	-	-	instr / rot?
307993483	HD 73990	B7/8V	5221605085661325056	0.40	-0.07	-	-	$\beta$ Cep ? / SPB
308395911	HD 66591	B4V	5479669466951012224	-1.33	-0.15	2	F	SPB
308454245	HD 67420	B9V	5275660856854591360	0.39	0.07	-	-	$\delta$ Sct
308456810	HD 67170	B8III/IV	5289613208437434240	0.05	0.04	-	-	rot?
308537791	HD 67277	B8III	5290024533163062144	0.18	-0.01	-	-	rot
308748912	HD 68423	B6V	5277219758184463488	-0.74	-0.06	-	-	SLF? / outburst? / instr
309702035	HD 271163	B3Ia	4660142634076536320	-3.61	-0.03	-	-	SLF
313934087	HD 224990	B3/5V	2320885329010329216	-1.32	-0.19	4/18	F/X	SPB / rot
327856894	HD 225253	B8IV/V	4701860922688030720	-0.80	-0.14	3/109	F/U	rot? / outburst? / instr?
349829477	HD 61267	B9/A0IV	5292390815325246976	1.07	0.09	-	-	const?
349907707	HD 61644	B5/6IV	5289291395127135360	-0.35	0.23	-	-	EB + puls
350146577	HD 63204	ApSi	5288156497263051136	0.65	-0.03	-	-	rot

Table 1 continued

Table 1 (continued)

TIC	Name	Sp. Type SIMBAD	Gaia DR2 ID	$M_G$ (mag)	BP - RP (mag)	# Spectra	Instrument	Var. Type
350823719	HD 41037	B3V	5275962500997316864	-0.88	-0.23	5/6	F/U	SPB? / rot
354671857	HD 14228	B8IV	4936685751335824896	0.15	3.16	10/79	F/U	SPB? / rot
355141264	HD 208495	B9.5V	6561093750492347136	1.30	-0.03	-	-	const?
355477670	HD 220802	B9V	6525840590207613824	0.34	-0.09	8	F	const?
355653322	HD 224686	B8V	6485326438580933888	-0.74	-0.07	52	F	rot? / outburst? / instr?
358232450	HD 6882 A	B6V+B9V	4913847589156808960	0.10	-0.18	24/33	F/U	EB
358466708	CD-60 1931	B7	5290739387520374912	-0.04	-0.01	-	-	rot / SPB
358467049	CPD-60 944 AB	B8pSi	5290722929205920640	0.18	0.06	-	-	rot
358467087	CD-60 1929	B8.5IV	5290722860486442752	0.36	0.13	-	-	SPB / EV? / rot? / SLF? / instr?
364323837	HD 40031	B6III	4758153203612698624	-1.44	-0.13	4	F	rot? / SPB?
364398190	CD-60 1978	B8.5IV-V	5290816009737675392	0.64	0.05	-	-	rot? / SLF?
364398342	HD 66194	B3Vn	4776318613169946624	-2.36	-0.33	97	U	rot? / SPB? / Be
364421326	HD 66109	B9.5V	5287999576341359360	-0.18	0.08	-	-	rot?
369457005	HD 197630	B8/9V	6681797793393053696	0.44	-0.11	1/15	F/U	rot / SPB?
370038084	HD 26109	B9.5/A0V	4666380781970681472	1.65	0.19	-	-	const?
372913233	HD 65950	B8III	5290671733195996416	-1.20	0.06	5	F	const? / outburst? / instr?
372913582	CD-60 1954	B9.5V	5290725643625189504	0.29	0.11	-	-	const? / outburst? / instr?
372913684	HD 65987	B9.5IVpSi	5290820682661822848	-0.67	-0.02	-	-	rot
373843852	HD 269525	B0I	4658678973606061696	-2.39	-0.32	-	-	SPB? / rot?
389921913	HD 270196	B1.5Ia	4662413606586588160	-2.83	0.09	1/8	F/U	SLF
391810734	HD 269655	B0Ia	4661289630893455488	-2.51	-0.11	2	F	SLF
391887875	HD 269660	B2Ia	4657362548954664192	-3.36	-0.14	-	-	SLF
404768847	VFTS 533	B0Ia	4651835308326981504	-1.95	-0.06	-	-	SPB? / SLF?
404768956	CI* NGC 2070 Mel 12	B0.5Ia	4658479691454645504	-2.91	0.03	-	-	SLF? / SPB? / instr?
404796860	HD 269920	B3Ia	4657652476416109184	-3.84	0.04	-	-	SLF
404852071	Sk-69 265	B3I	4660612881443486720	-2.93	-0.09	-	-	SLF
404933493	HD 269997	B2.5Ia	4660135826507549824	-3.14	-0.06	1	F	SLF
404967301	HD 269992	B2.5Ia	4657636675267019008	-3.51	0.18	2	F	SLF
410447919	HD 64811	B4III	-	-	-	-	-	rot/SPB?
410451677	HD 66409	B8IV/V	5290769211774211968	0.32	0.05	4	F	rot

Table 1 continued

Table 1 (*continued*)

TIC	Name	Sp. Type SIMBAD	Gaia DR2 ID	$M_G$ (mag)	BP - RP (mag)	# Spectra	Instrument	Var. Type
419065817	HD 1256	B6III/IV	2364986843479227392	0.13	-0.13	-	-	rot / SPB?
425057879	HD 269676	O6+O9	4651834616802932608	-1.79	-0.20	-	-	instr.? / binary? / rot?
425081475	HD 269700	B1.5Iaeq	4657685534828270976	-2.78	0.33	1/48	F/X	SLF / rot.? / Be
425083410	HD 269698	O4Ia	4660121743354291328	-2.38	-0.34	6	U	rot / SPB? / SLF?
425084841	TYC 8891-3638-1	BIIa	4658474743652257664	-3.93	0.04	2/6	F/U	SLF
441182258	HD 210934	B7V	6618669608159645312	-0.53	-0.14	-	-	instr / SPB/outburst?
441196602	HD 211993	B8/9V	6615398767225726848	0.46	-0.09	2/9	U/X	const?
469906369	HD 212581 AB	B9Vn+G0V	6404338508023617664	-0.10	-0.03	19	U	SPB / $\beta$ Cep / instrumental?

## B. TESS LIGHT CURVES AND AMPLITUDE SPECTRA

In this section, we provide the light curves and amplitude spectra for the 154 O and B stars observed by TESS in sectors 1 and 2 at a 2-min cadence. This appendix will be available electronically.